CrystEngComm

RSC Publishing

PAPER

View Article Online
View Journal | View Issue



Cite this: *CrystEngComm*, 2013, **15**, 1989

# Single crystal growth and characterization of tetragonal $FeSe_{1-x}$ superconductors

Dmitriy Chareev,[a] Evgeniy Osadchii,[a] Tatiana Kuzmicheva,[b] Jiunn-Yuan Lin,[c] Svetoslav Kuzmichev,[d] Olga Volkova[d] and Alexander Vasiliev*[d]

Received 14th November 2012,
Accepted 4th January 2013

DOI: 10.1039/c2ce26857d

www.rsc.org/crystengcomm

The plate-like single crystals of tetragonal (*P4/nmm*) $FeSe_{1-x}$ superconductors were grown using the KCl–$AlCl_3$ flux technique which produced single crystalline tetragonal samples of about 4 × 4 × 0.1 $mm^3$ dimensions. The energy dispersive X-ray spectroscopy established a ratio of Fe : Se = 1 : 0.96 ± 0.02. The resistivity and magnetization measurements revealed a sharp superconducting transition at $T_c$ = 9.4 K. Multiple Andreev reflections spectroscopy pointed to the existence of two-gap superconductivity with the gap values $\Delta_L$ = 2.4 ± 0.2 meV and $\Delta_S$ = 0.75 ± 0.1 meV at 4.2 K.

## Introduction

Iron-based superconductors are extremely sensitive to impurity phases and defects in the crystal structure, which could significantly change the physical and chemical properties both in normal and superconducting states.[1] This vulnerability is due to the fact that both microscopic and macroscopic inhomogeneities could be magnetically active, therefore influencing bulk and surface superconductivity. In the basic families of iron superconductors, the 11-type materials stand apart, owing to the absence of intermediate charge reservoir layers. The $FeSe_{1-x}$ compounds consist only of a stack of electronically active layers weakly coupled by the van der Waals interaction. These layers are based on the edge-shared $FeSe_4$ tetrahedra. $FeSe_{1-x}$ demonstrates superconductivity with $T_c \geqslant$ 8 K,[2–4] but its single crystals can be used for either production of intercalated materials $A_xFe_2Se_2$ (A = Li, Na, Ba, Sr, Ca, Yb and Eu) with $T_c$ = 30–46 K[5] or superconducting monolayers with $T_c$ = 65 K.[6–8] In this paper we describe the synthesis of $FeSe_{1-x}$ single crystals from the halide eutectic flux under steady temperature gradient conditions and provide proofs of their high quality by the measurements of transport and thermodynamic properties.

The superconducting tetragonal phase of $FeSe_{1-x}$ exists only below 730 K (457 °C) in a rather narrow composition range.[9] If these conditions are not fulfilled, the samples are contaminated by Fe, $Fe_7Se_8$, and $Fe_3O_4$ impurities.

The attempts to grow tetragonal $FeSe_{1-x}$ single crystals from alkali–halide flux have been undertaken in ref. 10–13. The synthesis of iron selenides from KCl flux with the melting temperature 776 °C was described in ref. 10. The ampoule with Fe, Se and flux was heated up to 840 °C and sustained at this temperature for 30 hours (h) to homogenize the solution. It was then cooled down to 820 °C for 1 h to provide the necessary supersaturation for nucleation. Further cooling was done with the rate of 0.3–0.5 °C $h^{-1}$ from 820 to 770 °C. After that, the ampoule was cooled rapidly down to 400 °C and held for 24 h to stabilize Fe and Se. The single crystals with the hexagonal shape were produced in this synthesis. Ref. 11 presented the synthesis based on NaCl/KCl flux with the eutectic temperature 657 °C. The ampoule with preliminary obtained $FeSe_{0.89}$ powder and flux was heated to 900 °C. Three steps of cooling were employed: firstly with 3 °C $h^{-1}$ rate down to 740 °C, secondly with 1 °C $h^{-1}$ rate down to 600 °C, and, finally, the furnace was cooled rapidly down to room temperature. Structural measurements revealed that both tetragonal (α) and hexagonal (β) phases coexist in the sample. A more promising method with LiCl–CsCl mixture which melts at 326 °C was used in ref. 12. The ampoule with elemental Fe and Se mixed with the flux was heated to 715 °C, and kept for 1 h at this temperature before shifting to a preheated furnace at 457 °C. After slow cooling down to 300 °C it was quenched in water. The main disadvantage of this method is that it likely results in either α or β phase depending on the various growth conditions. Application of vapor transport method to the synthesis of tetragonal $FeSe_{1-x}$ in ref. 13 also had the same problem as above. Therefore, to grow tetragonal $FeSe_{1-x}$ single crystals of high quality, it is necessary to use a eutectic flux which melts at low temperatures (preferably below 250 °C),

[a]*Institute of Experimental Mineralogy, Russian Academy of Sciences, 142432 Chernogolovka, Moscow District, Russia*
[b]*P.N. Lebedev Physical Institute, Russian Academy of Sciences, 119991 Moscow, Russia*
[c]*Institute of Physics, National Chiao Tung University, Hsinchu 300, Taiwan, R.O.C*
[d]*Low Temperature Physics and Superconductivity Department, M.V. Lomonosov Moscow State University, 119991 Moscow, Russia. E-mail: vasil@mig.phys.msu.ru; Fax: +07 495 9329217; Tel: +07 495 9329217*

and to synthesize at temperatures below 457 °C to obtain reproducible growth results.

## Experimental section

The $FeSe_{1-x}$ single crystals were grown from the flux under a permanent gradient of temperature. The chemical compositions of tetragonal $FeSe_{1-x}$ and hexagonal $Fe_7Se_8$ were studied by energy-dispersive X-ray spectroscopy performed on a CAMECA SX100 (15 kV) analytical scanning electron microscope. The X-ray diffraction spectra were collected by a DRON diffractometer (Co Kα-radiation, Fe filter) in the $10^\circ < 2\theta < 90^\circ$ range on the powder samples prepared by grinding small or medium sized single crystals in acetone. To compare the quality of obtained single crystalline samples an additional amount of polycrystalline iron selenide was prepared by the conventional solid-state reaction.[13] The FeSe single crystals X-ray diffraction spectra were collected along the *c*-axis using a BRUKER diffractometer (CuK$\alpha_1$ radiation, graphite monochromator).

The $FeSe_{1-x}$ single crystals were grown in evacuated quartz ampoules using a KCl–$AlCl_3$ flux.[14] The temperature of synthesis and phase compositions were chosen in accord with the Fe–Se phase diagrams.[9] It is noted that the tetragonal $FeSe_{1-x}$ phase easily coexists with hexagonal $Fe_7Se_8$ phase and pure iron. The decomposition of $FeSe_{1-x}$ tetragonal phase to $Fe_7Se_8$ and Fe occurs at temperatures above 457 °C (730 K). The homogeneity range of tetragonal $FeSe_{1-x}$ is very narrow, *i.e.*, from $FeSe_{0.96}$ to $FeSe_{0.975}$.[15]

The starting chemicals were carbonyl iron powder or iron spheres with the diameter of about 0.2 mm, crystalline selenium purified by the floating zone method, potassium chloride KCl and anhydrous aluminum chloride $AlCl_3$ (Fluka, 98%). The iron powder and pieces of selenium were mixed in the ratio Fe : Se = 1 : ~0.94 and loaded into silica ampoules with an inner diameter of 8 mm and length of 110 mm. Then hygroscopic $AlCl_3$ was promptly weighed in air and loaded into the ampoules. Finally, KCl taken in the ratio $AlCl_3$ : KCl = 2 : 1 was weighed and added into the ampoules which were evacuated down to $10^{-4}$ bar pressure and sealed. The ampoules with chemicals were loaded into a horizontal tube furnace, heated to the temperature of synthesis for 1–2 h, and then kept at this temperature for 40–50 days. The temperature of the hot part of the ampoules was about 700–740 K. That of the cold part was 650–680 K. The volume fraction of the melted eutectic from the volume of sealed ampoules was about 60–65%.

The ampoules were eventually extracted from the furnace and cooled in air. The cold part of the ampoules with crystals of iron selenide was cut off and the eutectic retrieved from it was dissolved in distilled water. Then, the crystals were rinsed in an ultrasonic bath twice in alcoholand twice in acetone. The rinsed crystals were dried in a muffle furnace at 70 °C for a few minutes. Tetragonal crystals were separated using a steel magnetic filling knife which can attract metallic iron and hexagonal $Fe_7Se_8$. Cleaning the crystals in water and alcohol did not produce any visible oxidation of the surface. The crystals were placed into evacuated silica glass ampoules for further physical characterization.

The temperature dependence of magnetization of $FeSe_{1-x}$ single crystals was measured by a ''Quantum Design'' SQUID magnetometer MPMS – 9 T. Transport properties of $FeSe_{1-x}$ were measured by a standard four-probe method. The superconducting gap values in $FeSe_{1-x}$ were determined by superconductor–normal metal–superconductor (SnS) Andreev spectroscopy. This method is based on multiple Andreev reflections effect[16] occurring in ballistic junctions of a SnS-type. ''Ballistic'' implies the contact diameter $a$ to be larger than the quasiparticle mean free path $l$.[17] To realize the experimental method, SnS contacts were formed in $FeSe_{1-x}$ samples by a ''break-junction'' technique.[18] The samples (thin plates with dimensions $2 \times 1 \times 0.1$ mm$^3$) were attached with two current and two potential leads to the sample holder by a liquid In–Ga alloy; the holder was then cooled down to liquid helium temperature $T = 4.2$ K. Forthcoming precise bending of the sample holder causes a microcrack generation into the sample: the microcrack was in fact a contact between two cryogenic clefts separated with a constriction. The layered structure of $FeSe_{1-x}$ implies exfoliation of the single crystals along the *ab*-planes, which provides easy mechanical readjustment of the contact point, forming tens of contacts during an experiment. The microcrack location deep into the sample prevented any impurity presence at clean cryogenic clefts and the overheating of the junction.

## Composition, crystal structure and morphology

The shape of the crystals was characterized by scanning electron microscope images shown in Fig. 1–3. Tetragonal single crystals with dimensions $4 \times 4 \times 0.1$ mm$^3$ with well shaped habitus were obtained at a temperature gradient of 710–660 K, as shown in Fig. 1 and 2. On the contrary, the samples prepared at higher temperatures, *i.e.* at a temperature gradient of 730–680 K, had an imperfect shape, nonstable chemical composition, and were mixed with the hexagonal $Fe_7Se_8$ impurity phase, as shown in Fig. 3. The chemical composition of tetragonal $FeSe_{1-x}$ phase was found to be $x \sim 0.04 \pm 0.02$. The hexagonal phase was identified to be $Fe_7Se_8$ from the energy-dispersive X-ray analysis. No additional impurity ions, *i.e.* K, Al or Cl, were found in iron selenides.

The phase purity and quality of $FeSe_{1-x}$ single crystals were established by indexing the X-ray diffraction patterns. All peaks in the X-ray diffraction pattern of the single crystals ground in an agate mortar, shown in Fig. 4a, were ascribed to tetragonal *P*4/*nmm* (129) unit cell, $a = 3.765$ Å, $c = 5.518$ Å, $V = 78.2(2)$ Å$^3$. These values are in correspondence with those reported in ref. 19. The X-ray diffraction pattern of $FeSe_{1-x}$ single crystal represents only the (*00l*) reflexes, as shown in Fig. 4b. While the X-ray diffraction pattern of the polycrystal-

 

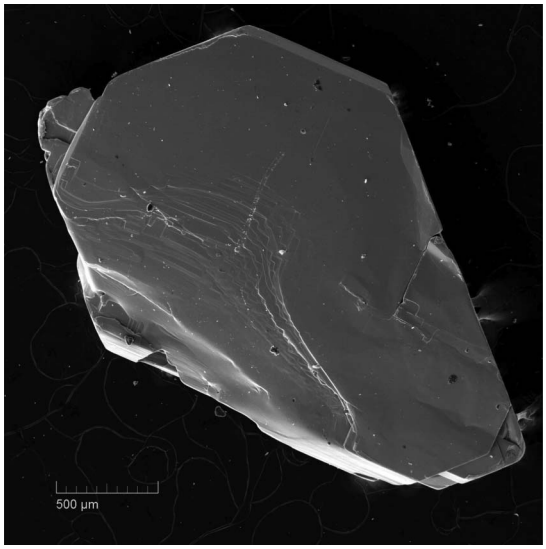


**Fig. 1** The scanning electron microscope image of a tetragonal $FeSe_{1-x}$ single crystal.

line sample synthesized for comparison by the solid-state reaction contains the peak attributed to an $Fe_3O_4$ impurity phase in Fig. 4c.

A possible explanation for the absence of $Fe_3O_4$ impurities in the samples prepared from KCl–$AlCl_3$ is in its transformation to soluble form by the reaction:

$$3Fe_3O_4 + 3Fe + 8AlCl_{3(liq)} = 4Al_2O_3 + 12FeCl_{2(liq)}$$

Therefore, the high quality of $FeSe_{1-x}$ single crystals was achieved primarily due to the application of the eutectic melt of salts including fusible aluminum chloride, and secondly due to the growth conditions of a permanent gradient of

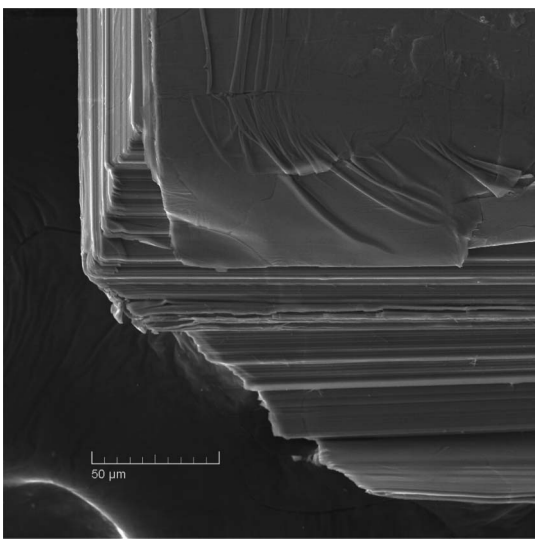


**Fig. 2** The scanning electron microscope image of the layered structure of a tetragonal $FeSe_{1-x}$ single crystal.

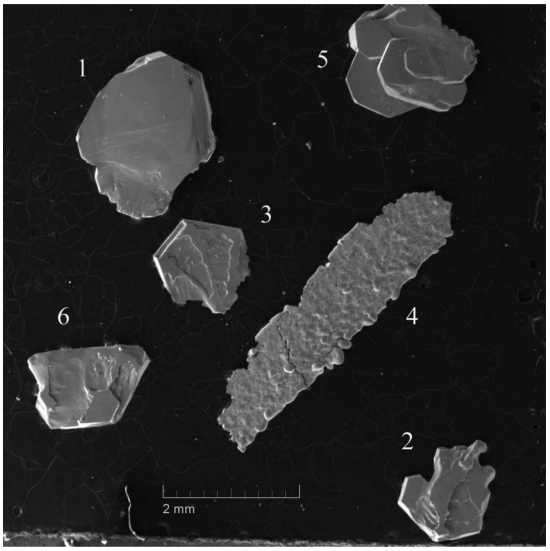


**Fig. 3** The scanning electron microscope images of the products obtained at high temperatures. 1, 2, 3, 6 – hexagonal $Fe_7Se_8$ crystals; 4 – hexagonal $Fe_7Se_8$ crystals 5 – a tetragonal $FeSe_{1-x}$ crystal.

temperature. The use of $AlCl_3$–KCl eutectic mixture with the melting temperature lower than 150 °C allows the transport of both iron and selenium at temperatures much lower than that

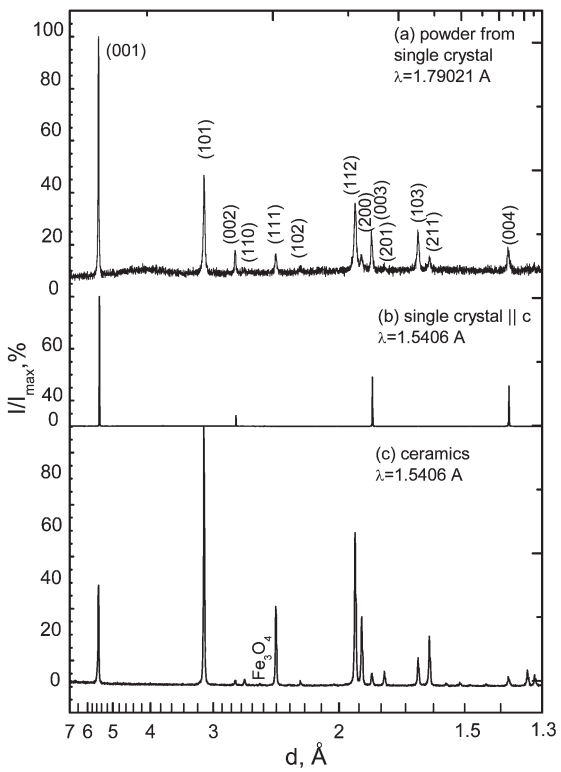


**Fig. 4** The X-ray diffraction patterns of tetragonal $FeSe_{1-x}$. Panel a represents the X-ray diffraction pattern of the single crystals ground in an agate mortar (Co Kα). Panel b represents the X-ray diffraction pattern along the *c*-axis (Cu $K\alpha_1$). Panel c represents the X-ray diffraction pattern of the polycrystalline sample synthesized by the solid-state reaction (Cu $K\alpha_1$).

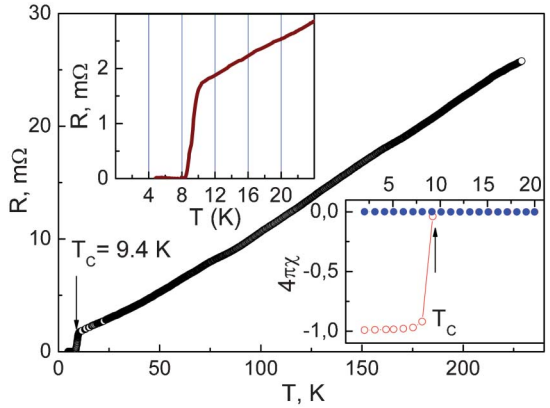


**Fig. 5** The temperature dependence of resistance of a $FeSe_{1-x}$ single crystal. The lower inset shows the temperature dependence of magnetic susceptibility measured in the magnetic field $B \| c$ = 20 Oe in both ZFC (open circles) and FC (closed circles). The upper inset shows the enlarged superconducting transition region.

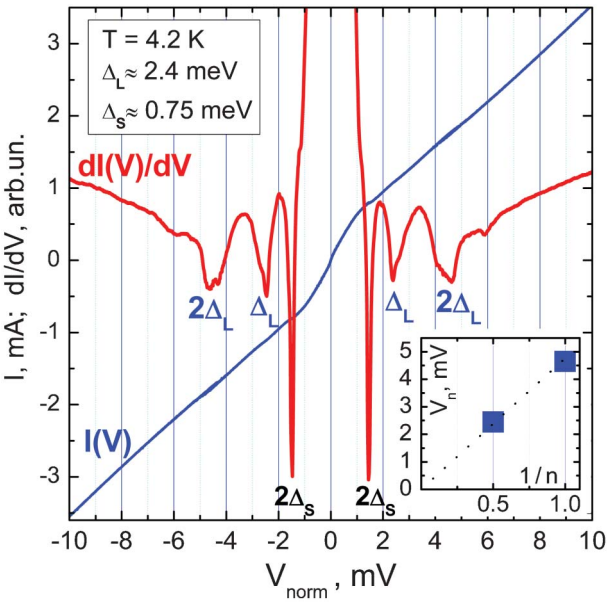


**Fig. 6** Current–voltage characteristic (thin blue line) and dynamic conductance (bold red line) measured at $T$ = 4.2 K for SnS-Andreev contact. Andreev dip positions define the large gap value $\Delta_L \approx 2.4$ meV (the corresponding minima are marked as $2\Delta_L$ and $\Delta_L$) and the small gap $\Delta_S \approx 0.75$ meV ($2\Delta_S$ labels). Inset shows a linear dependence of the large gap minima voltages $V_n$ *versus* $1/n$.

of the dissociation of tetragonal FeSe (457 °C). Besides, application of $AlCl_3$–KCl mixture instead of CsCl–LiCl flux prevents lithium from reacting with quartz ampoules. The permanent gradient of temperatures allows growth of single crystals under well defined conditions as compared to that upon slow cooling of the melt.

## Transport and magnetic properties

The quality of $FeSe_{1-x}$ single crystals was examined by physical measurements. The temperature dependence of resistance $R(T)$, shown in Fig. 5, demonstrates a metallic behavior with $T_c$ = 9.4 K. This $R(T)$ also indicates the high quality of the FeSe single crystal. For example, the kink at 90 K manifests the structural phase transition. The width of superconducting transition amounts to 1.5 K (see upper inset to Fig. 5). Magnetic measurements confirm the presence of the superconducting phase transition around 9.4 K (lower inset to Fig. 5). Magnetic properties show a nearly 100% Meissner effect.

The superconducting gap values in $FeSe_{1-x}$ found from Andreev spectroscopy were analyzed according to Kümmel *et al.*[20] The current–voltage characteristic for an SnS contact exhibits an excess current at low bias and a subharmonic gap structure due to the multiple Andreev reflections effect, which reveals a series of minima for the dynamic conductance d$I(V)$/d$V$ at the bias voltages

$$V_n = \frac{2\Delta}{en}, n = 1, 2, 3, \ldots \quad (1)$$

where $\Delta$ is a superconducting gap value, $e$ the elementary charge, $n$ the subharmonic order. The relative intensity of the Andreev peculiarities decreases exponentially with increasing $n$. For a two-gap superconductor, such structures should appear in d$I(V)$/d$V$ of the SnS contact.[21] Using eqn (1), one can directly obtain a gap value from the corresponding Andreev minima positions without any fitting.

The experimental current–voltage characteristic in Fig. 6 (thin blue line) with an excess current at low bias voltages is typical for the clean classical SnS-Andreev contact. Therefore, the constriction exercises normal metal properties, and the theory by Kümmel *et al.*[20] is applicable to the present break-junctions. Dips of the contact dynamic conductance (the bold red lines in Fig. 6) located at $V_{L1} \approx \pm 4.6$ meV ($n$ = 1; marked as $2\Delta_L$) and $V_{L2} \approx \pm 2.4$ meV ($n$ = 2; marked as $\Delta_L$), in accord with eqn (1), can be considered as the first and the second Andreev reflexes. Eqn (1) implies a linear dependence of Andreev dip positions *versus* their reversed number, $V_n(1/n)$, starting at (0;0) point. Such a dependence was plotted for the large gap dynamic conductance dips (inset of Fig. 6). The experimental points do follow eqn (1) and suggest the large gap $\Delta_L$ = 2.4 ± 0.2 meV. This large gap value is not far from the maximum value of 2.0 meV of the anisotropic gap found in the specific heat data.[22] The next peculiarities located at $V_{S1} \approx \pm 1.5$ meV ($2\Delta_S$ labels) do not correspond to the expected third Andreev minima positions for the large gap as their intensity is much higher than that of the second dips for the large gap. Therefore, the minima located at $V_{S1} \approx \pm 1.5$ meV indicates a new subharmonic gap structure, associated with the small gap $\Delta_S$ = 0.75 ± 0.1 meV. Dynamic conductance for several SnS contacts has been studied in the same way and the results are consistent. The peculiarities sharpness confirms a good quality of the single crystals due to the microscopic homogeneity.

 

The value of $2\Delta_L/k_BT_C \approx 5.9 \pm 1$ exceeding the BCS value of 3.52 is close to those obtained in other works[4,23,24] using FeSe monolayers, poly- and single crystals.

## Conclusions

We present the method for the growth of high quality $FeSe_{1-x}$ single crystals in $KCl–AlCl_3$ eutectic mixture under conditions of a permanent gradient of temperature of 385–427 °C. We also found that better quality of the samples can be achieved at lower temperatures. Physical characterizations indicates a superconducting state below 9.4 K. SnS-Andreev spectroscopy shows two superconducting gaps with $\Delta_L = 2.4 \pm 0.2$ meV and $\Delta_S = 0.75 \pm 0.1$ meV. The large gap BCS-ratio of $2\Delta_L/k_BT_C \approx 5.9 \pm 1$ points to strong coupling in FeSe.

## Acknowledgements

The authors thank T.N. Dokina, K.V. Van, A.A. Viryus, A.N. Nekrasov for technical support and Ya.G. Ponomarev for valuable discussions. This work was supported by a grant of the President of the Russian Federation for State Support of Young Russian Scientists (MK-1557.2011.5), and the Russian Foundation for Basic Research 12-02-90405, 12-02-90823, and Russian Ministry of Science and Education 11.519.11.6012 and 8378.

## References

1 D. C. Johnston, *Adv. Phys.*, 2010, **59**, 803.
2 F. C. Hsu, J. Y. Luo, K. W. Yeh, T. K. Chen, T. W. Huang, P. M. Wu, Y. C. Lee, Y. L. Huang, Y. Y. Chu, D. C. Yan and M. K. Wu, *Proc. Natl. Acad. Sci. U. S. A.*, 2008, **105**, 14262.
3 Y. Mizuguchi, F. Tomioka, S. Tsuda, T. Yamaguchi and Y. Takano, *Appl. Phys. Lett.*, 2008, **93**, 152505.
4 B. Büchner and C. Hess, *Nat. Mater.*, 2009, **8**, 615.
5 T. P. Ying, X. L. Chen, G. Wang, S. F. Jin, T. T. Zhou, X. F. Lai, H. Zhang and W. Y. Wang, *Sci. Rep.*, 2012, **2**, 426.
6 R. Schneider, A. G. Zaitsev, D. Fuchs and H. v. Löhneysen, *Phys. Rev. Lett.*, 2012, **108**, 257003.
7 L. Li, Z. R. Yang, Y. P. Sun, J. Y. Zhang, D. Z. Shen and Y. H. Zhang, *Supercond. Sci. Technol.*, 2011, **24**, 015010.
8 D. Liu, W. Zhang, D. Mou, J. He, Y.-B. Ou, Q.-Y. Wang, Z. Li, L. Wang, L. Zhao, S. He, Y. Peng, X. Liu, C. Chen, L. Yu, G. Liu, X. Dong, J. Zhang, C. Chen, Z. Xu, J. Hu, X. Chen, X. Ma, Q. Xue and X.-J. Zhou, *Nat. Commun.*, 2012, **3**, 931.
9 H. Okamoto, *J. Phase Equilib.*, 1991, **12**, 383.
10 S. B. Zhang, X. D. Zhu, H. C. Lei, G. Li, B. S. Wang, L. J. Li, X. B. Zhu, Z. R. Yang, W. H. Song, J. M. Dai and Y. P. Sun, *Supercond. Sci. Technol.*, 2009, **22**, 075016.
11 R. Hu, H. Lei, M. Abeykoon, E. S. Bozin, S. J. L. Billinge, J. B. Warren, T. Siegrist and C. Petrovic, *Phys. Rev. B: Condens. Matter Mater. Phys.*, 2011, **83**, 224502.
12 U. Patel, J. Hua, S. H. Yu, S. Avci, Z. L. Xiao, H. Claus, J. Schlueter, V. V. Vlasko-Vlasov, U. Welp and W. K. Kwok, *Appl. Phys. Lett.*, 2009, **94**, 082508.
13 G. Kullerud, Experimental techniques in dry sulfide research in *Research Techniques for High Pressure and High Temperature*, ed. G. C. Ulmer, Spinger-Verlag, New York, 1971, pp. 288–315.
14 G. H. Moh and L. A. Taylor, *Neues Jahrb. Mineral., Monatsh.*, 1971, **10**, 450.
15 F. Gronvold, *Acta Chem. Scand.*, 1968, **22**, 1219.
16 A. F. Andreev, *J. Exp. Theor. Phys.*, 1964, **19**, 1228.
17 Yu. V. Sharvin, *J. Exp. Theor. Phys.*, 1965, **48**, 984.
18 J. Moreland and J. W. Ekin, *J. Appl. Phys.*, 1985, **58**, 3888.
19 G. Hägg and A. L. Kindstrom, *Z. Phys. Chem.*, 1933, **22**, 455.
20 B. Kümmel, U. Gunsenheimer and R. Nicolsky, *Phys. Rev. B: Condens. Matter*, 1990, **42**, 3992.
21 B. A. Aminov, A. A. Golubov and M. Y. Kupriyanov, *Phys. Rev. B: Condens. Matter*, 1996, **53**, 365.
22 J.-Y. Lin, Y. S. Hsieh, D. A. Chareev, A. N. Vasiliev, Y. Parsons and H. D. Yang, *Phys. Rev. B: Condens. Matter Mater. Phys.*, 2011, **84**, 220507.
23 M. Bendele, S. Weyeneth, R. Puzniak, A. Maisuradze, E. Pomjakushina, H. Luetkens, S. Katrych, A. Wisniewski, R. Khasanov and H. Keller, *Phys. Rev. B: Condens. Matter Mater. Phys.*, 2010, **81**, 224520.
24 Ya. G. Ponomarev, S. A. Kuzmichev, M. G. Mikheev, M. V. Sudakova, S. N. Tchesnokov, T. E. Shanygina, O. S. Volkova, A. N. Vasiliev and Th. Wolf, *J. Exp. Theor. Phys.*, 2011, **113**, 459.